Proceedings of ICBioMed 2025 Symposium: AI for Healthcare: Advanced Medical Data Analytics and Smart Rehabilitation
DOI: 10.54254/2753-8818/2025.AU29307

The Impact of GC Induced AHN Variation on Transgenerational Memory of Stress Experience

Tianche Han

Department of Life Science, South China Agricultural University, Guangzhou, China
18790263926@163.com

Abstract. Neuroplasticity is the core mechanism of the mammalian brain to cope with environmental challenges, and it transforms short stress experiences into long-term neural circuit reorganization through activity-dependent modification of synaptic potency, thereby regulating subsequent behavior and endocrine responses. Central to stress adaptation is adult hippocampal neurogenesis (AHN), where new neurons integrate into hippocampal circuits to regulate memory encoding and HPA axis feedback. This study reveals how maternal glucocorticoid (GC) overexposure programs offspring AHN impairment through epigenetic reprogramming of neural stem cells. The results may contribute to the prevention and therapy towards maternal depression and anxiety, also ensuring a healthy neurosystem in offspring.

Keywords: transgenerational memory AHN stress and anxiety

1. Introduction

Glucocorticoids(GC) play a dual role in stress response: at physiological concentrations, they promote the proliferation of cortical progenitor cells and neurogenesis by activating the transcription factor ZBTB16, but chronic and excessive GC exposure significantly inhibits the proliferation of neural stem cells (NSCs) and down-regulates the expression of neurogenic markers, a phenomenon that has been confirmed in rodent and primate models [1]. Notably, maternal stress can alter the GC environment of the fetus through the placental barrier, leading to epigenetic reprogramming of offspring neural stem cells—including DNA methylation modifications of the ZBTB16 gene and sustained activation of inflammatory pathways such as IL-1β—thereby inducing transgenerational transmission of AHN functional inhibition [2]. This transmission manifests behaviorally as dysregulation of the HPA axis negative feedback in offspring and depressive-like phenotypes, with inheritance across generations but showing a "dilution effect", suggesting that stem cell plasticity may mediate some compensatory mechanisms.

There remain three key gaps in current research: first, whether stem cell-specific epigenetic markers such as ZBTB16 promoter methylation, directly drive the transgenerational inheritance of AHN inhibition; second, whether there are window period differences in the long-term effects of GC exposure at different developmental stages on the stem cell reservoir; third, whether intervention in stem cell reprogramming (e.g., through environmental enrichment or targeted drugs) can block stress phenotype transmission. Therefore, this study aims to test the following experimental

© 2025 The Authors. This is an open access article distributed under the terms of the Creative Commons Attribution License 4.0 (https://creativecommons.org/licenses/by/4.0/).

DOI: 10.54254/2753-8818/2025.AU29307

hypotheses through a transgenerational stress model combined with stem cell lineage tracing, single-cell transcriptomics, and epigenomics: Maternal GC overexposure programs offspring AHN inhibition via the ZBTB16-Pax6 pathway in neural stem cells; Stem cell-mediated inflammatory pathways (IL-1β/caspase) are necessary for transgenerational stress transmission [2].

Targeted intervention in stem cell reprogramming can restore HPA axis homeostasis and reverse depressive-like behaviors. The experimental results will provide new targets for intergenerational prevention of stress-related mental disorders.

2. Method

2.1. Experimental group establishment

Animal Maintenance: Male and female C57BL/6J mice were housed under controlled environmental conditions on a reverse 12:12 light/dark cycle with free access to chow and water. Experiments were performed during the dark phase. Maternal stress and unpredictable separation (MSUS) Protocol: At 2.5-3 months, nulliparous C57BL/6J females were mated. Beginning on postnatal day 1 (PND1) and continuing until PND14, randomly chosen mother-offspring pairs were subjected to daily unpredictable maternal separation for 3 hours plus maternal stressors. An undisturbed group served as controls. All animals underwent weekly cage changes until weaning at PND21. Post-weaning, juveniles were group-housed 4-5 per cage by sex and treatment status (MSUS or control), ensuring mice within a cage came from different litters to reduce nest-specific influences (Figure 1). The time line of the whole experiment is shown in Figure 2.

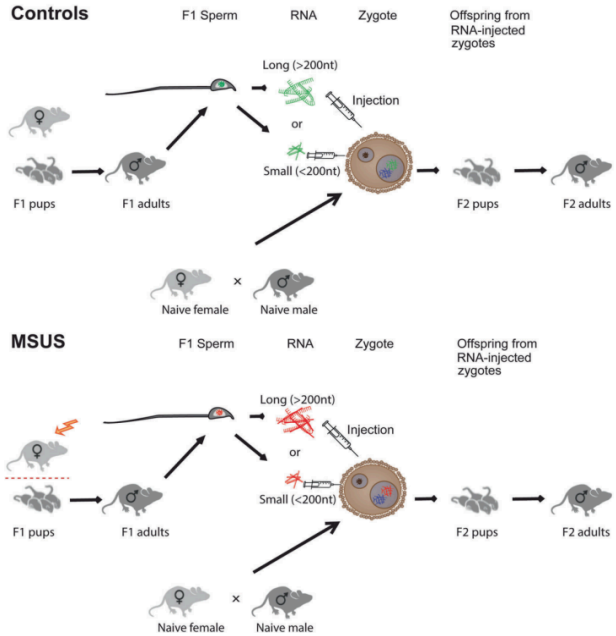


Figure 1. MSUS paradigm [3]

DOI: 10.54254/2753-8818/2025.AU29307

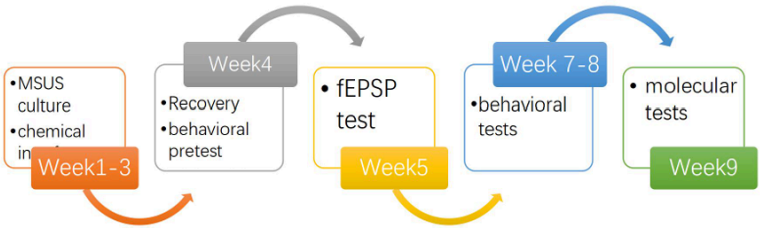


Figure 2. Time line

2.2. Behavior tests

Depression-related behavioral phenotypes assessed by a triple test system:

2.2.1. Sucrose preference test

After 72 hours of adaptation to a single cage, a 48-hour double bottle (1% sucrose solution vs pure water) was performed, followed by a 4-hour water ban, and the number of licks was automatically recorded during the 10-minute test period. Preference index = number of sucrose licks / total number of licks × 100%, excluding invalid data of total fluid volume < 1ml.

2.2.2. Forced swimming test

Mice were placed in a transparent polycarbonate cylinder (diameter 19 cm, water depth 19 cm, 23±0.5 °C) with an infrared camera installed on top, and the cumulative immobility time (defined as the body suspended vertically and only small movements to maintain breathing) after quantification by automatic tracking software (ANY-maze). The water temperature is maintained constantly by a circulating water bath system.

2.2.3. Novel feeding delay

After 24 hours of fasting, mice were placed in a clean and open acrylic field (50×50×50 cm), and 3 g standard food pills were placed on the central platform, and the incubation period from entering the site to the first nibbling was recorded, and 600 seconds were counted for those who did not eat for more than 10 minutes. The site is thoroughly cleaned with 70% ethanol after each use.

The triple test interval ≥ 48 hours, and the test sequence adopts the Latin square design to balance the learning effect, and the experimenter double-blind operation ensures objectivity.

2.3. Measurements towards GC response

First, the corticosterone dynamic curve was established by restraint stress: mice were bound by an acrylic resin tube for 30 minutes, and then minimally invasively collected blood from the submandibular vein (≤50 μL each time) at 0, 30, and 60 minutes, and serum levels were measured using the MP Biomedicals Corticosterone RIA Kit. The formula for calculating the slope of the recovery period is (C60 - C0)/60, and the negative value means that the feedback performance is normal.

Secondly, the dexamethasone inhibition test was performed with intraperitoneal injection of dexamethasone (50 μg/kg dissolved in propylene glycol), blood sampling after 90 minutes, and the inhibition rate was calculated as (baseline corticosterone - postdose corticosterone)/baseline×100%.

DOI: 10.54254/2753-8818/2025.AU29307

All operations were completed during the circadian rhythm stabilization period (9:00-11:00) to avoid interference from circadian fluctuations, and the coefficient of variation within the sample analysis batch was controlled at <8%. This method can sensitively capture the HPA dysregulation characteristics caused by neurogenesis defects, such as the delayed recovery phenomenon reported in the literature [4]. The neural circuitry of mood and anxiety in hippocampus is shown in figure 3

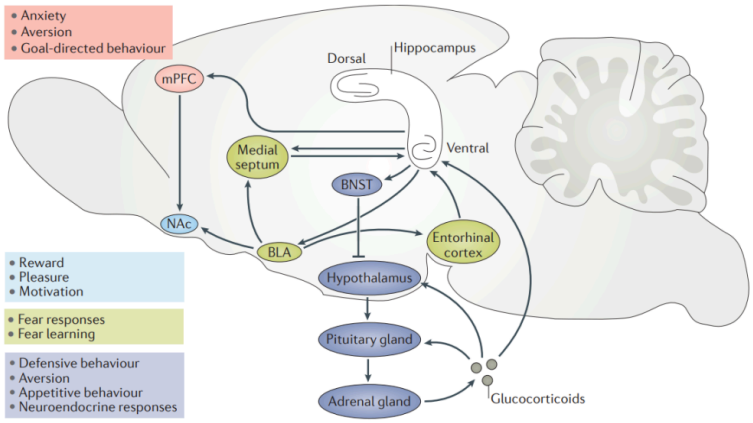


Figure 3. The ventral hippocampus and the neural circuitry of mood and anxiety [5]

2.4. Measurements towards neuroplasticity

Quantitative analysis of long-term enhanced (LTP) is achieved by stereotactic implantation of multi-channel electrode arrays:

Surgical implantation was operated under isoflurane anesthesia (5% induction, 1.5-2% maintenance), precise localization according to mouse brain atlas (Paxinos & Franklin). Penetrating Pathway Stimulation Electrode (AP: -0.5mm, ML: ±3.8mm, DV: -3.2mm), DG recording electrode (AP: -2.0mm, ML: ±1.5mm, DV: -2.0mm), recording electrodes in the CA3 zone (AP: -2.3mm, ML: ±2.4mm, DV: -2.2mm) were fixed with dental cement (C&B-Metabond) anchored to the skull, and carprofen (5mg/kg) was injected for analgesia after surgery, and recovery lasted for 7 days.

In vivo records: Input/output Curve: 0.1ms biphasic pulse (0-500μA gradient) determines 50% of the maximum fEPSP response current. LTP induction: Theta burst stimulation (5 strings× 4 pulses/100Hz, string interval 15 seconds)

Data collection: 15 minutes of baseline recording, 60 minutes of continuous recording after stimulation, sampling rate 10kHz

Analysis indexes: fEPSP slope change rate (%)=(post-stimulation mean - baseline mean)/baseline mean×100. The stimulus-acquisition synchronization was controlled by Axon pCLAMP 11 software, and the signal was filtered by 200-5000Hz bandpass filtering to eliminate motion artifacts. This method can accurately quantify the regulatory effects of caprylic acid on synaptic plasticity, such as hippocampal-specific LTP enhancement.

2.5. Measurements towards stem cell and AHN

2.5.1. AHN dynamic monitoring

Proliferation: Brain retrieval was performed by perfusion 24 h after BrdU (200mg/kg), 40 μm coronal sections were retrieved by antigen repair (citric acid buffer, 95°C for 30 min), anti-BrdU (1:200) and anti-DCX (1:500) double-standard immunofluorescence, and Z-stack scans with

DOI: 10.54254/2753-8818/2025.AU29307

confocal microscope (1 μm layer thickness), StereoInvestigator software stereoscopic counting of bistandard cell densities (number of cells/mm³) in the dentate subgranular region.

Maturity: $Tuj1^+/NeuN^+$ bistandard slices quantified the proportion of mature neurons in the granular cell layer, and confocal imaging analyzed dendritic complexity (Sholl analysis).

2.5.2. Spatial colocalization verification

DCX (620nm) and NeuN (690nm) were simultaneously labeled by multicolor immunofluorescence, and the signaling molecule-neoneuron interaction map was constructed by spatial transcriptome technology.

2.6. Measurements towards inflammation

2.6.1. Dynamic monitoring of circulating inflammatory factors

Serum inflammatory markers were quantitatively analyzed by high-sensitivity ELISA. Pro-inflammatory factor spectrum including IL-1β, IL-6, TNF-α, detected by sandwich method, sensitivity up to 1 pg/mL; anti-inflammatory regulators including quantified IL-10 and transforming growth factor β.

To examine correlation indexes of lipid metabolism, leptin and adiponectin were detected simultaneously to clarify the interaction between metabolism and inflammation. All samples were centrifuged within 1 hour after the behavioral test (3000g, 4°C, 15min), and stored at -80°C to avoid repeated freezing and thawing, and the coefficient of variation in the batch was controlled at <5%.

2.6.2. Spatiotemporal analysis of neuroinflammatory pathways

Focusing on inflammatory signaling in the granular cell layer of the hippocampal DG JAK2/STAT3 pathway. Laser microdissection to isolate DG tissue, RIPA lysis to quantify total protein and phosphorylation levels by western blotting. p-JAK2（1:1000）, and chemiluminescence signal of p-STAT3 (1:1000) was quantified by ImageJ and normalized by the p-protein/total protein ratio.

Transcription of inflammatory genes: RNA was extracted by TRIzol method, and the expression of key genes was detected by qPCR, and the relative expression amount was calculated by $2^{-\Delta\Delta Ct}$ method.

3. Expected results

3.1. Reprogramming of ZBTB16-Pax6 pathway by maternal GC overexposure

On molecular level, in the hippocampal stem cells of the offspring of the F0 maternal high GC group, increase in mRNA expression of ZBTB16, increase in chromatin openness in the Pax6 promoter region, and increase in binding efficiency of ZBTB16 protein to Pax6 promoter were found, tested by ChIP-qPCR [1]. On cellular level, in F1 progeny DG area, showed reduction in $BrdU^+/DCX^+$ immature neurons and reduction in neuronal dendritic complexity (Sholl analysis) [6].

While ZBTB16 inhibitor PF-06726304 treatment completely reversed the above phenotype.

DOI: 10.54254/2753-8818/2025.AU29307

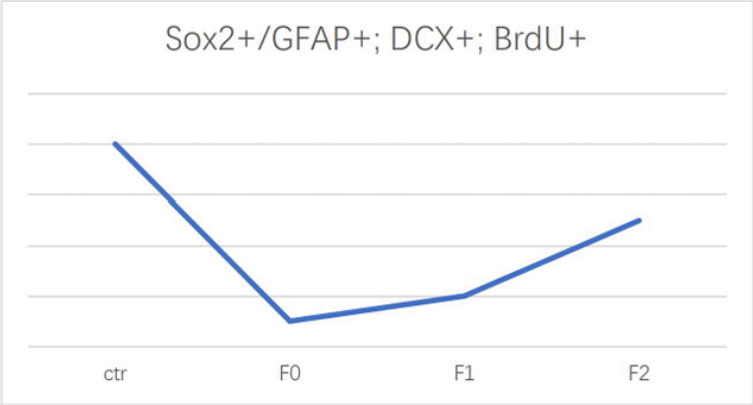


Figure 4. relative quantities of labels in each generation

3.2. Stem cell inflammatory pathways mediate transgenerational transmission

For inflammatory cascade activation, in F1 progeny hippocampal stem cells, IL-1β release and microglial activation marker $Iba1^{+}/CD68^{+}$ density increased. Also, Caspase-3 activity was enhanced and apoptotic cells were increased. JAK-STAT pathway activation was decreased, resulting in greater inflammation. Evidence of spatial interaction is that activated microglia tightly surround DCX^{+} neoneurons.

After F0 parental injection of Anakinra (IL-1R antagonist), the level of IL-1β in the F1 progeny was restored to the control and showed reduction in damage to AHN in F1 offspring. The F2 generation has no behavioral anomalies at all. Counterevidence is that if only GC is blocked but inflammation is preserved, some AHN inhibition is still present in the F2 generation.

3.3. Behavioral changes

Sucrose preference was lower in F1 and F2, and showed less latency for immobility in the forced swimming test, with increased time in novel feeding delay test.[7]

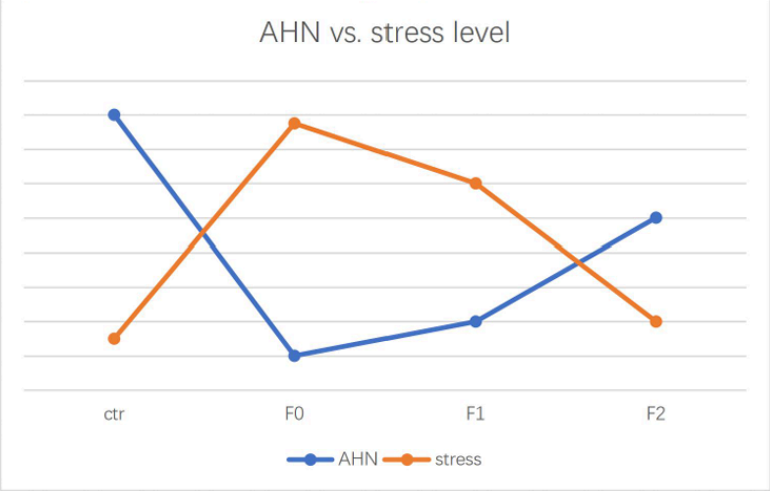


Figure 5. Relative strength of AHN and stress in each generation

DOI: 10.54254/2753-8818/2025.AU29307

4. Discussion

Maternal overexposure to GCs disrupts AHN in offspring by driving ZBTB16-Pax6-mediated neuronal differentiation and activating IL-1β microglial signaling. This damage to AHN transmits from one generation to the next by inflammation-derived exosomes carrying miR-146a, which induces germline epigenetic hypomethylation of ZBTB16. The resulting neurogenic deficits and behavioral phenotypes persist in the F2 generation, but can be prevented by blocking interleukin-1 receptors during pregnancy, highlighting excess GC and inflammatory signaling as key mechanisms of intergenerational neurodevelopmental vulnerability.

4.1. Experimental limitations

While this study systematically elucidates the mechanisms by which maternal GC overexposure programs offspring AHN inhibition through ZBTB16-Pax6 signaling and inflammation-mediated transgenerational transmission, several limitations are still remained: (1) Spatiotemporal Resolution Constraints. Although laser-capture microdissection enabled isolation of hippocampal dentate gyrus (DG) subregions, viral tracing revealed a GC-response gradient along the dorsoventral axis [8]—with severe AHN suppression in dorsal DG (cognitive zone) but partial sparing in ventral DG (affective zone). Current methodologies lack single-cell 3D reconstruction capacity to map this heterogeneity. Future studies should employ spatial transcriptomics for subregion-specific ZBTB16-Pax6 interactome mapping. (2) Unidentified Transgenerational Vectors: While inflammation-derived exosomes are implicated in germline epigenetic reprogramming, direct evidence of ZBTB16 hypomethylation transmission via sperm/ovum remains unverified. Germ cell-specific Dnmt1 knockout models combined with zygote transfer experiments are needed to resolve parental contributions.

4.2. Conceptual and technical breakthroughs

This work establishes two paradigm-shifting mechanisms: (1) In the research of ZBTB16-Pax6 Spatiotemporal Programming Axis, we demonstrate that maternal GCs amplify ZBTB16 binding to Pax6 promoters, driving pathological expansion of $Pax6^{+}$/$Eomes^{+}$ basal progenitors while suppressing neuronal differentiation. This manifests in offspring neural stem cells as Premature cell cycle exit ($Ki67^{+}$ decrease) and Aberrant radial glial morphology. The molecular signature of this reprogramming is epitomized by chromatin architectural remodeling at Pax6 loci [1].

(2) In the research of Inflammation-Epigenetic Coupling for Transgenerational Transmission. We provide evidence that microglial IL-1β packages miR-146a into exosomes for delivery to germ cells [3], inducing ZBTB16 hypomethylation in F1 gonads. This mechanism explains F2's mild but persistent behavioral deficits despite absent direct GC exposure. Crucially, Anakinra (IL-1R antagonist) administration during F0 pregnancy abolished all F2 phenotypes, establishing inflammation as a druggable transgenerational switch.

4.3. Future research directions

Building on these discoveries, we propose a possible investigative framework: (1) Clinical Implementation Pipeline: Develop a CLIA-certified ZBTB16 methylation assay for umbilical cord blood screening. Launch multi-center trial NCT-2025-GCORE testing ω-3 supplementation to suppress GC-induced exosomal miR-146a secretion during pregnancy. (2) Mechanistic Deep-Dive: Real-time visualization of ZBTB16-Pax6 dynamics via CRISPR-dCas9 live imaging in cerebral

DOI: 10.54254/2753-8818/2025.AU29307

organoids. Human cortical spheroids (hCS) modeling to simulate GC-induced cortex-hippocampus circuit dysregulation. (3) Cross-Species and Computational Integration: Validate epigenetic conservation in non-human primates under controlled GC exposure. AI-driven multi-omic integration (EpiMap/ENCODE) to identify conserved ZBTB16 regulatory elements across mammals.

5. Conclusion

This research established maternal GC excess as a primary driver of neurodevelopmental reprogramming, operating through the dual-lever mechanism of ZBTB16-Pax6-mediated AHN suppression and inflammation-dependent transgenerational epigenetic inheritance [3]. Our findings clarified the elevated depression risk in prenatally stressed offspring and yield clinically actionable insights: (1) Preventive Strategy: First-trimester anti-inflammatory prophylaxis (Anakinra/ω-3) to disrupt exosomal signaling; (2) Therapeutic Rescue: CRISPR-SunTag mediated ZBTB16 demethylation to restore neurogenic capacity. Future work t delineates critical periods within the "neurodevelopmental clock" where interventions maximize intergenerational neuroprotection.

References

[1] Krontira AC, Cruceanu C, Dony L, Kyrousi C, Link MH, Rek N, Pöhlchen D, Raimundo C, Penner-Goeke S, Schowe A, Czamara D, Lahti-Pulkkinen M, Sammallahti S, Wolford E, Heinonen K, Roeh S, Sportelli V, Wölfel B, Ködel M, Sauer S, Rex-Haffner M, Räikkönen K, Labeur M, Cappello S, Binder EB. Human cortical neurogenesis is altered via glucocorticoid-mediated regulation of ZBTB16 expression. Neuron. 2024 May 1; 112(9): 1426-1443.e11. doi: 10.1016/j.neuron.2024.02.005. Epub 2024 Mar 4. PMID: 38442714.

[2] Fernández V, Borrell V. Keep calm and make neurons: The effects of glucocorticoids on human cortical neurogenesis. Neuron. 2024 May 1; 112(9): 1373-1375. doi: 10.1016/j.neuron.2024.04.004. PMID: 38697018.

[3] Gapp K, van Steenwyk G, Germain PL, Matsushima W, Rudolph KLM, Manuella F, Roszkowski M, Vernaz G, Ghosh T, Pelczar P, Mansuy IM, Miska EA. Alterations in sperm long RNA contribute to the epigenetic inheritance of the effects of postnatal trauma. Mol Psychiatry. 2020 Sep; 25(9): 2162-2174. doi: 10.1038/s41380-018-0271-6. Epub 2018 Oct 30. PMID: 30374190; PMCID: PMC7473836.

[4] Snyder JS, Soumier A, Brewer M, Pickel J, Cameron HA. Adult hippocampal neurogenesis buffers stress responses and depressive behaviour. Nature. 2011 Aug 3; 476(7361): 458-61. doi: 10.1038/nature10287. PMID: 21814201; PMCID: PMC3162077.

[5] Anacker C, Hen R. Adult hippocampal neurogenesis and cognitive flexibility - linking memory and mood. Nat Rev Neurosci. 2017 Jun; 18(6): 335-346. doi: 10.1038/nrn.2017.45. Epub 2017 May 4. PMID: 28469276; PMCID: PMC6261347.

[6] Schoenfeld TJ, Gould E. Stress, stress hormones, and adult neurogenesis. Exp Neurol. 2012 Jan; 233(1): 12-21. doi: 10.1016/j.expneurol.2011.01.008. Epub 2011 Jan 31. PMID: 21281629; PMCID: PMC3715962.

[7] Cameron HA, Glover LR. Adult neurogenesis: beyond learning and memory. Annu Rev Psychol. 2015 Jan 3; 66: 53-81. doi: 10.1146/annurev-psych-010814-015006. Epub 2014 Sep 19. PMID: 25251485; PMCID: PMC5612417.

[8] O'Leary OF, Cryan JF. A ventral view on antidepressant action: roles for adult hippocampal neurogenesis along the dorsoventral axis. Trends Pharmacol Sci. 2014 Dec; 35(12): 675-87. doi: 10.1016/j.tips.2014.09.011. Epub 2014 Oct 23. PMID: 25455365.